ELSEVIER

Journal of Structural Geology 30 (2008) 710–718

JOURNAL OF STRUCTURAL GEOLOGY

www.elsevier.com/locate/jsg

Influence of structural anisotropy on creep of rocksalt from Simla Himalaya, India: An experimental approach

R.K. Dubey [a,*], V.K. Gairola [b]

[a] *Department of Applied Geology, Indian School of Mines University, Dhanbad 826 004, India*
[b] *51/3 Hirdwar Road, Dehradun 248001, India*

Received 13 June 2007; received in revised form 7 December 2007; accepted 10 January 2008
Available online 18 January 2008

Abstract

The influence of structural anisotropy on time-dependent deformation (creep) of rocksalt from Shali Formation (Precambrian), Himachal Pradesh, India was investigated to analyze the differential mobility of rocksalt body in nature. The effect of structural anisotropy (orientation of bedding planes) with respect to the compression axis on the compressive strength, yield strength, modulus of elasticity, failure strain and yield strain of rocksalt has been analyzed on cubic samples ($5 \times 5 \times 5$ cm^3) to collect the basic input for the purpose of creep of rocksalt. Time-dependent compression of cubic samples perpendicular, parallel and oblique to bedding planes were subjected to constant stresses equal to 30%, 40%, 50%, 60%, 70%, 75%, and 80% of their uniaxial compressive strengths for presenting analogous situation of variable stressing of rocksalt caused by over laying rocks and tectonic stresses. The results of experimental deformation reveal the strong control of structural anisotropy on development of instantaneous strain, transient strain, steady-state strain and accelerated strain; however the influence of structural anisotropy on deformation of rocksalt decreases with increment in stress levels. At higher stress level creeps, the control of structural anisotropy on deformation became negligible. The progress of time-dependent deformation occurs due to evolution of minute tensile and shear crack arrays in proportions. At lower stress creep the development of tensile crack arrays and shear crack arrays is assisted by structural anisotropy. However, at higher stress levels the creep of rocksalt is facilitated by reduction in tensile crack arrays and domination of shear crack arrays, resulting in shearing where the anisotropic rocksalt exhibits isotropic behaviour. Thus the mobility of rocksalt bodies is dependent on characteristic of structural anisotropy and stress conditions.

Keywords: Structural anisotropy; Rocksalt; Creep; Constant stress level

1. Introduction

Deformation of rocks pertains to certain kinds of fracture-assisted geological structures and processes. The stress-induced formation of fractures in rocks often support open biochemical and physicochemical systems that play an important role in accumulation of hydrocarbons, formation of mineral deposits, extrusive and intrusive magmatic structures, precipitation of seismic events, etc., by participating in tectonic cycles (Pyrak-Nolte, 1996). The anisotropic rocks exhibit variation in mechanical properties with inclination of bedding planes and foliations measured from stress axis (Badgley, 1964; Donath, 1964; LeComte, 1965; McLamore and Gray, 1967; Horino and Ellickson, 1970; Lama and Vutukuri, 1978; Jaroszewski, 1984; Sheorey, 1997; Cristescu and Hunsche, 1998). Under compression the rocks compressed parallel and oblique to bedding and foliation planes exhibited slightly lower (Horino and Ellickson, 1970; Attewel and Sandford, 1974; Lama and Vutukuri, 1978; Jaroszewski, 1984; Ramamurthy et al., 1993) or higher (Cristescu and Hunsche, 1998) compressive failure stress than that obtained when compressed perpendicular to the bedding plane. However, under tensile stresses the rocks showed minimum ultimate stress,

* Corresponding author. Tel.: +91 9431711058 (mobile); fax: +91 326 220 3645.
E-mail addresses: rkdbhumin1085@yahoo.co.in, rkdubey1085@hotmail.com (R.K. Dubey), vkgairola@sify.com (V.K. Gairola).

0191-8141/$ - see front matter © 2008 Published by Elsevier Ltd.
doi:10.1016/j.jsg.2008.01.007

yield stress and modulus of elasticity when deformed perpendicular to the bedding (Jaroszewski, 1984) and the failure stress of the rock increased with the decrease in the inclination angle between the bedding plane and maximum tensile stress axis (Lama and Vutukuri, 1978). Mechanically the anisotropy is classified as inherent and induced anisotropy (Aubertin et al., 1991, 1993, 1996) or ''intrinsic'' and ''extrinsic'' anisotropies (Cristescu and Hunsche, 1998). The planar anisotropy is defined as ratio between the effective viscosities in pure and simple shear (Weijermars, 1992). Thus, rheological properties of the rock not only depend on the rock types (mineral constituents) but also on the types and density of the anisotropies present in them. The peak stress of the rock reduces with the increase in damage factor caused by induced anisotropy (Hongliang and Ahrens, 1994). However, Ramamurthy et al. (1993) suggested that the structural anisotropy does not play an effective role when the least principal stress is equal to the normal failure stress of the rocks. Koyi (1996, 1998) has attempted the simulation of anisotropic overburden on rocksalt layer in his analog modeling experiment to study the evolution of rocksalt in the Gulf of Mexico. For this purpose he has defined the anisotropy as the ratio between viscosity of material in shortening/extension parallel to layering and viscosity of material in shear parallel to layering, and being dependent on strain rates. At higher strain rate of deformation the anisotropy approaches unity, thus behaves isotropically in character (Koyi, 1996, 1998). Similarly, Dubey and Gairola (2000) have observed that in rocks the effect of structural anisotropy reduces with the increase in stress levels, and at a stress level of 72% of its compressive failure stress the structural anisotropy becomes ineffective in cyclic compression. Koyi and Sans (2006) have used lateral rheologic contrast (mechanical anisotropy) to suggest the possible impact on dominating hinterland-verging structures. Similarly, Bonini (2007) has simulated anisotropy of strata in the light of rheological stratigraphy in his analog modeling approach to study the deformation pattern and structural vergence in brittle–ductile thrust wedge.

The anisotropy and heterogeneity produced by fractures (bedding/foliations) can vary in time along with change in stress, temperature and pressure, and inherent constituents and fabrics of the rocks. Thus ''time'' plays an important role in deformation of rocks and irreversible deformation of rocks in domain of time is known as ''creep''. The creep is an important mechanism of deformation of rocks in ductile shear zones and numbers of metamorphosed zones of higher temperature and pressure (amphibolite and granulite facies). Besides tectonic stresses, anisotropy shows strong control over monotonic, quasistatic and creep deformations by affecting the mechanical properties of rocks. Creep experiments on basalt, sandstone, limestone, marbles, rocksalt, claystone, etc. have been carried out to study the effects of composition, textural and structural anisotropies (Griggs, 1939, 1940; Griggs et al., 1960; LeComte, 1965; Hansen, 1988; Skrotzki and Haasen, 1988; Pouya, 1991; Dubey, 1996; Dubey and Gairola, 2000, 2005). Rocksalt principally consisting of halite exhibits viscoelastic properties and flows easily along at least five independent active slip planes out of 12 possible slip planes (Cristescu and Hunsche, 1998). Thus it simulates rock material at great depth where it exhibits viscoelastic, viscous and viscoplastic behavior (Dusseault, 1989). Therefore rocksalt can be utilized as natural model material for understanding the processes going on at great depth in the interior of the Earth's crust. Thus, time-dependent deformation experiments on basalt, sandstone, limestone, marbles and rocksalt have been carried out to study the effects of composition, textural and structural anisotropies (Hansen, 1988; Skrotzki and Haasen, 1988; Pouya, 1991; Carter et al., 1993; Dubey, 1996; Dubey and Gairola, 2000, 2005). According to Hansen (1988) the water-insoluble impurities in rocksalt are ineffective at higher stresses in the late stages of deformation. Pouya (1991) has classified rocksalt into three petrological classes, namely ''milky'', ''intermediate'' and ''phenoblastic''. The milky rocksalt exhibits 1.5 times higher creep strain than the impure coarse-grained rocksalt (Pouya, 1991). Dubey (1996) and Dubey et al. (1999) have worked on the rocksalt from Himachal Pradesh, India and observed that the milky rocksalt exhibited 2–2.5 times higher creep strain in compression than impure phenoblastic rocksalt.

The present paper is an experimental attempt to study the influence of structural anisotropy on creep rocksalt belonging to the Lower Shali Formation (Lower Precambrian) exposed around Guma, District Mandi, Himachal Pradesh, India.

2. Material

Brownish purple, hard and compact rocksalt exhibits well-developed bedding defined by alternate 1 to 1.8 cm thick halite layers and 1 to 2 mm thick layer of impurities consisting of clay, mud, quartz and marl. In the thick halite layers subangular to subrounded halite grains range from 125 to 350 μm in size and exhibit 10% floating grains, 30% point grain contacts, 43.5% line grain contacts and 17% concavo-convex and suture grain contacts (Dubey,1996).

The grains exhibit a tendency for a preferred dimensional orientation along the bedding and show the effects of dynamic recrystallization as revealed by the undulatory extinction and subgrain formation. The grain size of the water-insoluble impurities ranges from 20 to 25 μm.

Rocksalt is mainly composed of 78.84% sodium chloride (NaCl) and 18.92% of water-insoluble materials like quartz, clay, mud and marl. In minor constituents, magnesium chloride ($MgCl_2$) and calcium sulfate ($CaSO_4$) range from 2.14% to 2.74% and 0.81% to 0.80%, respectively. Iron oxide (Fe_2O_3), sodium bicarbonate ($NaHCO_3$) and titanium oxide (TiO_2) occur in trace amounts of 0.20–0.24%. The presence of sodium bicarbonate in rocksalt is strong evidence of its marine origin (Kerr, 1977; Dubey, 1996; Dubey et al., 1999; Dubey and Gairola, 2005).

Experiments were performed on cubic specimens $5 \times 5 \times 5\ cm^3$ cut from large rocksalt samples collected from the field. Two sets of cubes were prepared. In one set specimens the bedding plane was parallel ($0^\circ \pm 2^\circ$) to two opposite faces of the cube. In the second set of specimens the bedding plane made an angle of 30° ($\pm 2^\circ$) with two opposite

faces of the cube. Three sets of experiments were carried out. In the first set the specimens were axially compressed perpendicular to the bedding (SPR). In the second set the specimens were deformed parallel to the bedding (SPL). In the third set of experiments the bedding made an angle of 30° (±2°) with the compressive axis.

3. Methodology

The mechanical properties of rocksalt with respect to three orientation of structural anisotropy (bedding plane) have been determined under uniaxial compressive quasistatic testing on a close- loop servo-controlled Material Testing System (MTS). The cubic samples of rocksalt of dimension of 5 cm × 5 cm × 5 cm were prepared with the help of rock cutter machine of medium duty in an air-flushing medium. The specimens were prepared in such a way that the bedding planes in specimens were perpendicular (SPR), Parallel (SPL) and oblique (SPO) to the compression axis (σ_1) (Fig. 1a) These three categories of rocksalt specimens were initially deformed monotonically at the loading rate of $3.5 \times 10^3\ s^{-1}$ for the determination of some mechanical properties on MTS (Table 1). The stress–strain curves were plotted on abscissa and ordinate, respectively (Fig. 1b). The mechanical properties of rocksalt were determined from the stress–strain curve (Table 1). Further, a few cubic samples of prepared cubes of rocksalt were deformed in a medium-duty hydraulic creep rig at constant stress levels equal to 30%, 40%, 50%, 60%, 65%, 67%, 70%, 72%, 75% and 80% of their uniaxial compressive strengths (failure stress or peak stress). However, the mechanical lever type creep machine provides a suitable condition for constant stress, but is limited by its loading amount (Li and Xia, 2000). The hydraulic creep machine used in the present study is based on the thrust of piston pushes by oil pressure generated from oil pump. The calibration curve of such a hydraulic creep machine (Fig. 1) suggested the relationship between effective stress in kg cm^{-2} (y) and applied stress in kg/ cm^{-2} (x) (Fig. 2) as

$$y = 0.242x \tag{1}$$

The small differences were selected at higher stress levels to determine the fine spectrum of deformation of rocksalt in the domain of time. The stress–strain and time curves were prepared from the results of creep experiments (Figs. 3–5). The various stages and constants of the creep equation were also determined to study the effect of anisotropy on creep with variable stress conditions as normally observed in progressive deformation of rocks in domain of time as shown in a typical creep curve (Fig. 6).

The readings were taken manually between an interval of 1, 5 and 10 min in the initial stages of creep deformation and later on the observations were made at an interval of 1 to 2 h. Further, the readings were taken at an interval of 10, 5, 2 and 1 min when the specimens approached failure. The strain–time curves were made for the specimens subjected to stresses of 30–80% of their compressive strengths (σ_c) (Figs. 3–5).

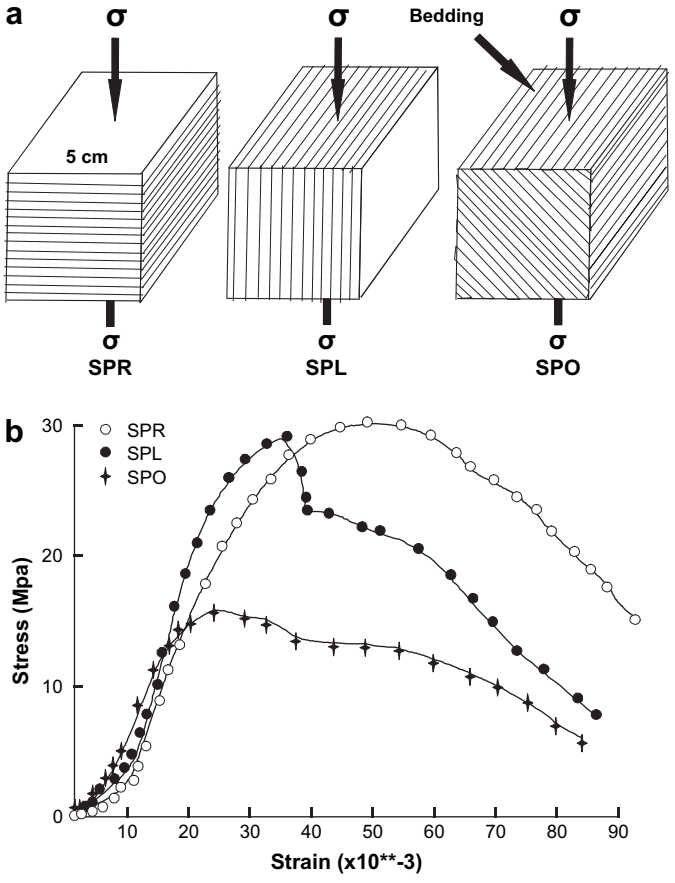

Fig. 1. (a) Structural anisotropy in rocksalt. (b) Stress–strain behaviour of three structural anisotropic classes of rocksalt from Guma, Mandi, H.P., India.

4. Results and discussion

The orientation of bedding with respect to compression axis (σ_1) direction exhibits a considerable bearing on the failure stress (compressive strength) (σ_c), yield stress (yield strength) (σ_y) and modulus of elasticity (E), failure strain and yield strain (Table 1). The rocksalt specimens compressed perpendicular to the bedding (SPR) showed highest uniaxial compressive strength (29.33 MPa), yield strength (20.05 MPa) and modulus of elasticity (1.804 GPa). The specimens compressed parallel to bedding (SPL) showed a nearly similar uniaxial compressive strength (28.08 MPa) and yield strength (16.54 MPa) and an intermediate modulus of elasticity (1.25 GPa) (Dubey and Gairola, 2000). However, specimens compressed oblique to the bedding (SPO) exhibited the least uniaxial compressive strength (15.62 MPa), yield strength (11.73 MPa) and modulus of elasticity (1.083 GPa). The variation in uniaxial compressive strength, yield strength and modulus of elasticity with respect to inclination of bedding due to compression direction showed a U shape (mechanical parameters show highest values in rocks containing inclination of bedding/foliation 90° from stress axis and progressively decrease with decrease in inclination of bedding/foliations up to inclination 32–45°, the value of mechanical parameters is

Table 1
The average values of mechanical properties of anisotropy classes of rocksalt from Guma, District Mandi, H.P.

Structural anisotropic classes	Compressive strength (failure stress (MPa)	Yield stress (MPa)	Modulus of elasticity (GPa)	Failure strain ($\times 10^{-2}$)	Yield strain ($\times 10^{-2}$)	Poisson's ratio
SPR	29.33	20.05	1.804	3.327	1.846	0.298
SPL	28.08	16.54	1.250	4.947	1.931	0.296
SPO	15.62	11.73	1.083	2.308	1.367	0.293

enhanced with reduction in inclination from 32° to 45° up to 0°). Similar results have been reported by Donath (1964), Horino and Ellickson (1970), Attewel and Sandford (1974), Ramamurthy et al. (1993), and Dubey and Gairola (2000). The observed pronounced difference in mechanical properties has been explained by Dubey and Gairola (2000). The higher values of uniaxial compressive strength and modulus of elasticity in the case of SPR and SPL may be attributed to the least shearing stress along the bedding planes. Slightly lower values of uniaxial compressive strength and modulus of elasticity in the case of SPL may be attributed to least shearing stress along the bedding planes. Slightly lower values of uniaxial compressive strength and modulus of elasticity in the case of SPL may be caused by the slight variation in the orientation of compression axis with respect to bedding planes. With progressive deformation and development of tensile stress normal to the bedding planes the specimen SPL shows slightly lower compressive strength and modulus of elasticity. However, in the case of SPO the bedding planes were oriented close to the plane of maximum shear stresses. Hence, SPO exhibited a lower value of uniaxial compressive strength and modulus of elasticity (Dubey and Gairola, 2000).

The strain–time curves of these three structural anisotropic classes (SPR, SPL and SPO) of rocksalt under various stresses exhibit a non-linear trend and show three stages of creep with instantaneous strain, transient creep and steady-state creep (Figs. 3–5). Besides, accelerated creep was also observed in some of the specimens. The rocks deformed at constant stress level exhibit instantaneous strain immediately just after loading due to elastic deformation; further, the development of strain at decreasing strain rates resulted in transient strain in rocks. The development of strain in rocks with decreasing strain rate ultimately reaches a constant value in the domain of time and thereafter the large amount of strain formed in rocks at constant strain rate, which is known as steady-state strain. After a long gap of time the rocks are subjected to higher strain, with an enhanced strain rate leading to failure of rocks due to formation of uncontrolled factures; this phase of creep is known as accelerated strain or dilation creep (Fig. 6). In the present experiment the instantaneous strain is smaller than the creep strain (transient creep and steady-state creep strains). The large creep strain developed in rocksalt results from the presence of at least five independent active slip planes amongst 12 slip planes in halite (chief constituent of rocksalt) (Cristescu and Hunsche, 1998). The halite belongs to the face-centered cubic crystals (FCC). The materials of the FCC system have 12 slip planes (Suresh, 1998), hence halite is characterized by 12 slip planes. The instantaneous strain (ε_i) is composed of instantaneous elastic strain (ε_{ie}) and instantaneous plastic strain (ε_{ip}) (Carter et al., 1993). The instantaneous strain in specimens compressed perpendicular to bedding (SPR) showed minimum instantaneous strain, whereas specimens compressed parallel to bedding (SPL) showed maximum instantaneous strain (Fig. 7). The larger instantaneous strain developed in SPL in comparison to instantaneous strain formed in SPR and SPL is caused by induced tensile stress acting perpendicular to the bedding planes and is attributed by least strength in tensile stress environment (Lama and Vutukuri, 1978). The specimens deformed perpendicular to bedding (SPR) showed least instantaneous strain due to the alignment of bedding planes in the direction of least

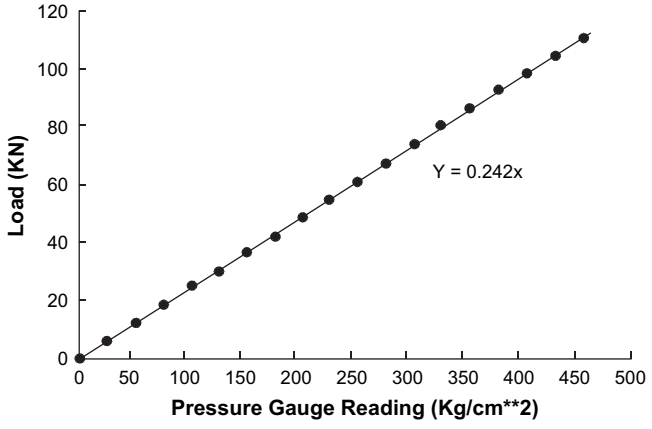

Fig. 2. Calibration curve of medium duty creep system.

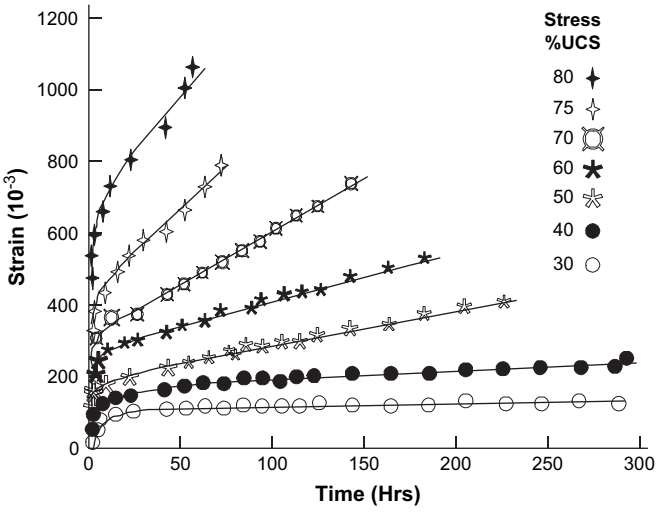

Fig. 3. Strain–time behaviour of rocksalt compressed perpendicular to bedding (SPR) at different constant stress levels.

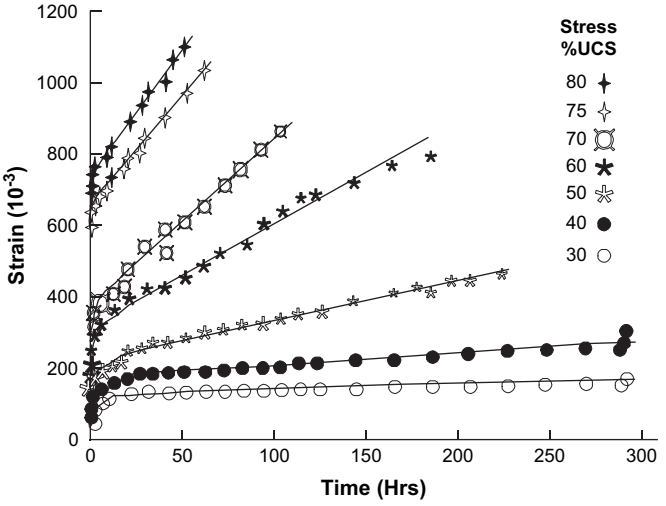

Fig. 4. Strain–time behaviour of rocksalt compressed parallel to bedding (SPL) at different constant stress levels.

induced tensile and shear stresses. The intermediate instantaneous strain developed in specimens deformed oblique to bedding planes (SPO) is caused by orientation of bedding planes close to natural shear planes. The small instantaneous strain developed in specimens SPR is evidence of higher modulus of elasticity of the specimen in comparison to modulus of the SPL and SPO (Table 1). The large instantaneous strain developed in SPL reveals the small value of modulus that is quite different from the modulus of elasticity determined from monotonic compression. However, the modulus of elasticity calculated from monotonic loading for SPO is the least but showed intermediate instantaneous strain; this may be due to sliding of cracked fragment along the bedding plane which resulted in reduction in the contact area of specimens with platens of the machine. The instantaneous strain increases with increase in stress level of creep, which shows a power relationship such as $\varepsilon_i = a \cdot \sigma^{\alpha}$ (Fig. 7, Eqs. (2)–(4)).

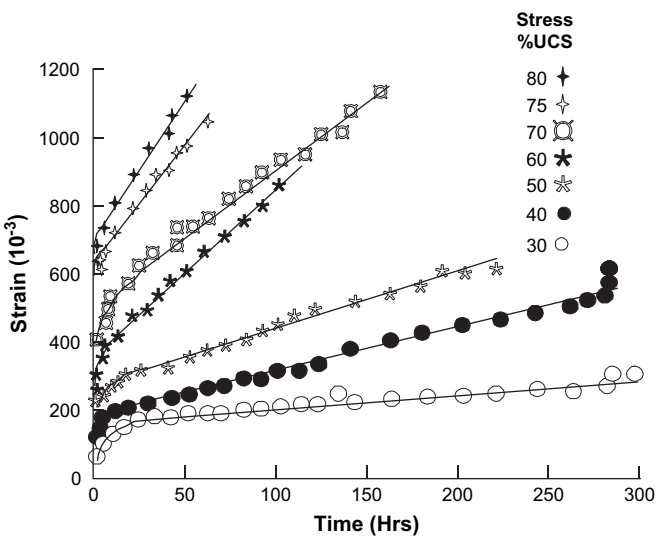

Fig. 5. Strain–time behaviour of rocksalt compressed oblique to bedding (SPO) at different constant stress levels.

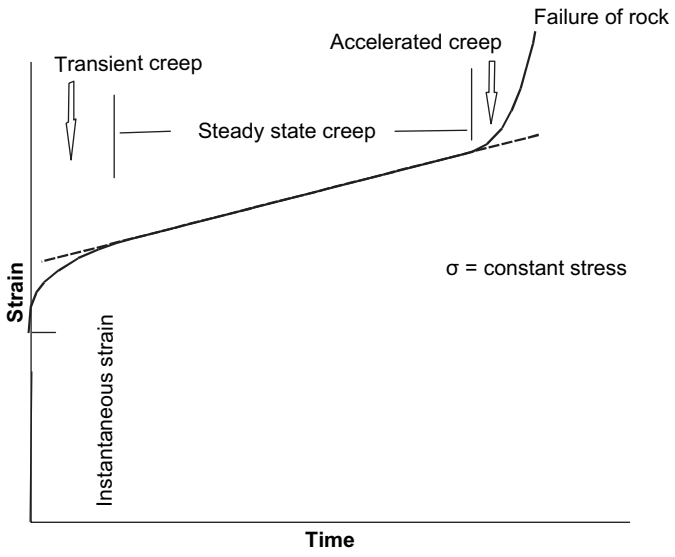

Fig. 6. A typical creep curve showing different stages of deformation of rocks.

$$\varepsilon_i^{SPR} = 0.0589\sigma^{1.8802} \quad (2)$$

$$\varepsilon_i^{SPL} = 0.079\sigma^{1.8557} \quad (3)$$

$$\varepsilon_i^{SPO} = 0.3215\sigma^{1.5581} \quad (4)$$

where ε_a is instantaneous strain and σ is stress level of creep. a is coefficient of power and α is exponent of power equations. The superscripts SPR, SPL and SPO are referred for three structural anisotropic classes of rocksalt. The coefficient of power (a) varies from 0.0589 to 0.3215 whereas the exponent of power (α) varies from 1.8802 to 1.5581. The specimen SPR showed the least value of a (0.0589) whereas specimen SPL was intermediate and SPO exhibited the highest value (0.3215). However, the specimen SPR showed the highest

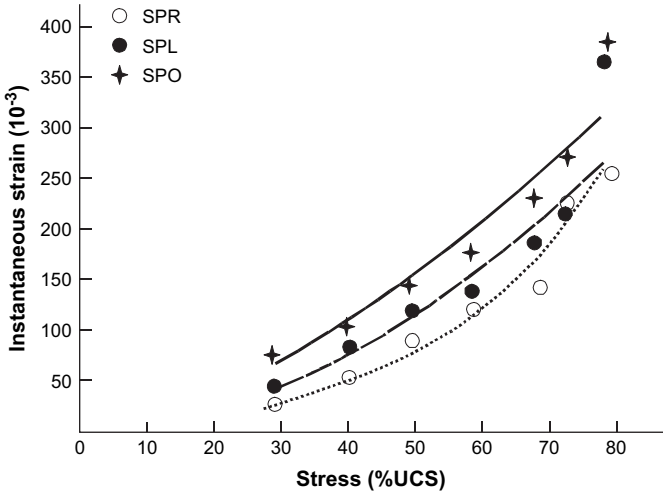

Fig. 7. Variation of instantaneous strain with change in constant stress levels in three structural anisotropic classes of rocksalt ($\varepsilon_i^{SPR} = 0.0589\sigma^{1.8802}$, $R^2 = 0.9908$; $\varepsilon_i^{SPL} = 0.079\sigma^{1.8557}$, $R^2 = 0.9308$; $\varepsilon_i^{SPO} = 0.3215\sigma^{1.5581}$, $R^2 = 0.9397$) from Guma, Mandi, H.P., India.

value of α (1.8802), SPL exhibited an intermediate value (1.8557) and SPO had the least (1.5581).

In the pronounced difference in coefficient of power a and exponent of power α in the case of SPO forming constants and exponents of SPR and SPL is evidence of shear slip along the inherent cracks, pore spaces and voids lying mainly along the bedding plane close to the shear plane. The slight difference in constant (a) and exponent (α) in the case of SPR and SPL is due to the effect of induced tensile stresses acting perpendicular to SPL, indicating there is no role of new anisotropy other than structural anisotropy. It is well known that the ratios of stress and instantaneous strains are generally linear in an elastic medium, but in the present study it is shown that a power trend may be due the viscoelastic nature of rocksalt. A number of rocks like sandstone, limestone, dolomite, etc. show a linear pattern of ratio of stress and instantaneous strain (Lama and Vutukuri, 1978; Dubey, 1996; Cristescu and Hunsche, 1998), but the rocksalt specimens exhibit a power fit and deviate from Hook's law given for a perfect elastic material due to viscoelestic behavior of rocksalt. The ratio of stress and instantaneous strain are also referred for modulus rocks. The modulus determined from stress and instantaneous strain is lower than the modulus of elasticity calculated from monotonic testing. The difference in modulus of specimens of rocksalt determined from creep test and monotonic loading is due to change in loading history. The difference in modulus of rocksalt is attributed to the slow impact of stress on specimens in the creep test, resulting in higher strain in comparison to strain formed in higher rate incremental stressing. This is supported by the well-defined higher modulus and strength of rocks at very high rate of stressing, i.e. under dynamic loading of order of wave frequency (Ranalli, 1995).

The SPR specimens exhibit the least transient creep due to attributes of opening of inherent cracks, pore spaces and voids lying parallel to beddings, and respond minimally to unfavorably oriented induced tensile stress (act parallel to bedding). The large transient creep developed in SPL is attributed by smooth opening of pre-existing cracks, pore spaces and voids lying along bedding planes in induced tensile stresses acting perpendicular to bedding planes (favorable for opening of cracks and voids). The SPO specimens showed an intermediate transient creep due to gradual chipping of specimens, resulting in reduced contact area of specimens with the platens of the machine. Pronounced variations have been observed in time duration of transient creep phase in specimens of three structural anisotropy classes of rocksalt (Fig. 8). The slope of the curve between time duration of transient phase and stress levels of creep showed a linear decreasing trend (Fig. 8, Eqs. (5)–(7)). The slope of the curve is highest negative in the case of SPR (−1.137) and least in the case of SPL (−0.6073). The slope of the curve is intermediate in the case of SPO (−0.8088). The least negative slope of the curve in the case of SPL is due to quick smooth opening of inherent crack pore spaces and voids deformed under induced tensile stresses acting perpendicular to bedding. The curves infer that the SPR specimens can survive in transient creep phase with small strain for a longer time at a constant stress than the SPO and SPL specimens.

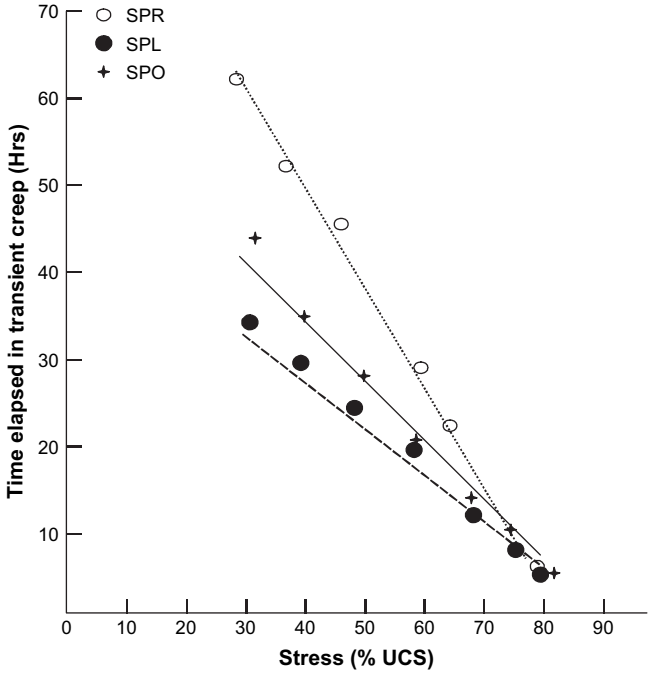

Fig. 8. Trend of time elapsed in transient creep along with variation in constant stress levels in three structural anisotropic classes of rocksalt ($t_{tr}^{SPR} = -1.1374\sigma + 97.332$, $R^2 = 0.9821$; $t_{tr}^{SPL} = -0.6073\sigma + 55.57$, $R^2 = 0.9891$; $t_{tr}^{SPO} = -0.8088\sigma + 70.145$, $R^2 = 0.9936$) from Guma, Mandi, H.P., India.

$$t_{tr}^{SPR} = -1.1374\sigma + 97.332 \quad (5)$$

$$t_{tr}^{SPL} = -0.6073\sigma + 55.57 \quad (6)$$

$$t_{tr}^{SPO} = -0.8088\sigma + 70.145 \quad (7)$$

where t_{tr} denotes time involved in transient creep phase, and superscripts SPR, SPL, and SPO denote classes of structural anisotropies.

Decrease in the duration of transient creep phase by increase in stress level of creep indicates the reduced effect of structural anisotropy on duration of transient creep phase. At 80% σ_c, the specimen SPO shows instantaneous strain and steady-state strain (ε_s) and transient creep completely vanishes. However, in the case of SPR and SPL the creep curves show all three stages of creep instantaneous strain, transient creep and steady-state creep, even at 80% σ_c (Li and Xia, 2000). Similar results have also been reported by Li and Xia (2000) for creep of claystone at 75% σ_c of stress level. Besides, the specimens SPR and SPL show a very small duration of transient creep phase, which may vanish at higher stress level of creep. Thus at a certain stress level of creep the transient creep may vanish and only instantaneous strain and steady-state creep playing a role in deformation of specimens may be due to development of a large plastic strain just after the specimens reach the instantaneous strain phase of creep.

The steady-state creep rate is highest in the case of SPO due to the large flow caused by alignment of bedding and new anisotropy close to shear plane. The steady-state creep rate is higher in the case of SPL than SPR due to the large flow that occurs by induced tensile stresses acting perpendicular to bedding in SPL. The SPR specimen exhibits small steady-state creep rate due to unfavorable conditions of induced tensile stresses parallel to bedding.

The increment in stress levels of creep results in an increase in increment in steady-state creep rate. Similar results have been also suggested from the experimental works carried out on various rocks (Attewel and Sandford, 1974; Skrotzki and Haasen, 1988; Pouya, 1991; Carter et al., 1993; Dubey, 1996; Cristescu and Hunsche, 1998; Maranini and Brignoli, 1999; Li and Xia, 2000). The steady-state creep rate increases as the stress level increases. The effect of stress level of creep has been observed to be maximal in the case of SPO due to alignment of structural anisotropy and induced anisotropy lying parallel to bedding that is close to the shear plane. The minimum steady-state creep rate in the case of SPR with respect to stress levels is caused by the least development of tensile stresses perpendicular and shear stresses oblique to the bedding plane. The plot between steady-state creep rate and stress level of creep infers a power relationship (Fig. 9, Eqs. (8)–(10))

$$\varepsilon_{st(SPR)} = 2E\text{-}09\sigma^{4.8751} \quad (8)$$

$$\varepsilon_{st(SPL)} = 5E\text{-}08\sigma^{4.1518} \quad (9)$$

$$\varepsilon_{st(SPO)} = 1E\text{-}05\sigma^{2.9688} \quad (10)$$

where ε_{st} denotes steady-state creep rate.

The constants of power relationship for steady-state creep rate in SPR, SPL and SPO are 2E-09, 5E-08 and 1E-05, respectively.

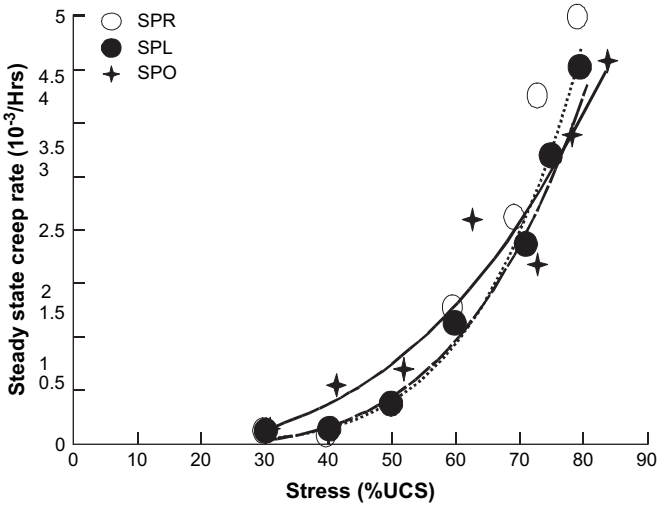

Fig. 9. Variation in steady-state creep rate with change in constant stress levels in three structural anisotropic classes of rocksalt ($\varepsilon_{st(SPR)} = 2E\text{-}09\sigma^{4.8751}$, $R^2 = 0.9356$; $\varepsilon_{st(SPL)} = 5E\text{-}08\sigma^{4.1518}$, $R^2 = 0.9859$; $\varepsilon_{st(SPO)} = 1E\text{-}05\sigma^{2.9688}$, $R^2 = 0.9512$) from Guma, Mandi, H.P., India.

At 80% σ_c all three structural anisotropy classes of rocksalt showed only instantaneous strain and steady-state creep due to a quick burst of inherent anisotropy exhibited by specimens at steady-state creep stage. The increase in steady-state creep is caused by increased applied stresses. The steady-state creep did not increase above 80% σ_c for SPR, 75% σ_c, for SPL and 70% σ_c, for SPO. At stress level of 80% σ_c the three structural anisotropic classes of rocksalt showed an almost equal rate of creep strain, However, the instantaneous strains are increased by an increase in creep stresses following Hook's law within the elastic limit before the initiation of stress induced new anisotropy (cracks). The differences in instantaneous strain as a result of elastic deformation strongly affected by the orientation of bedding planes can be explained as described earlier for the differences in short-term mechanical properties like uniaxial compressive strength, yield strength and modulus of elasticity. The equal rate of increase in steady-state creep results from formation of en-echelon crack array suggested by Lajtai et al. (1994) and Dubey and Gairola (2000) (Fig. 10). At lower stress levels the tensile crack array initiated along the bedding plane strikes perpendicular to the stress axis in the case of SPL (Fig. 10a). The formation of

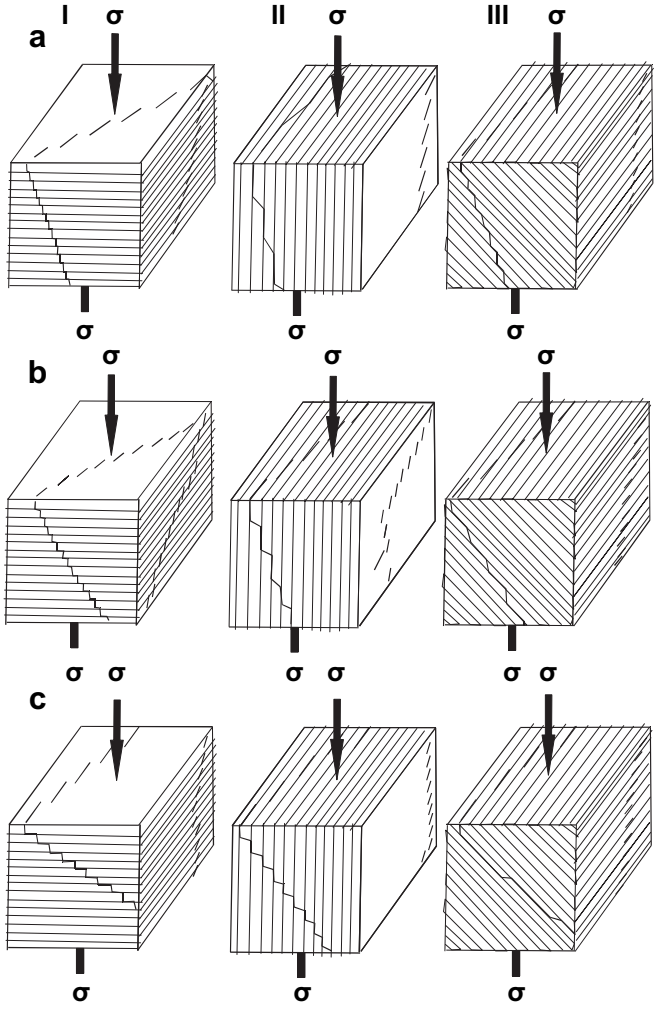

Fig. 10. Influence of structural anisotropy on evolution of various crack arrays pattern at different constant stress levels.

shear crack arrays along inclined bedding in SPO is due to inclination of natural shear plane near to the bedding (Fig10a III). The compression induced tensile stresses act at maximum perpendicular to bedding in SPL. In the case of SPR the shear crack array was initiated in small length across the bedding planes both in least tensile as well as shear stress along the bedding plane running perpendicular to the stress axis. The increment in stresses resulted in additional inclined crack wings to previously formed crack arrays, forming shear crack arrays in SPR (Fig. 10a I) and tensile crack arrays in SPO (Fig. 10 a III). In the case of SPR the tensile crack array was also formed but was short in length. At lower stress levels the length of tensile crack arrays are the longest in the case of SPL, and slightly shorter in SPR in comparison to SPL whereas it is much the shortest in the case of SPO, as a result of differences in steady-state creep rate of the three structural anisotropic classes of rocksalt. As the stresses of creep increase the tensile crack arrays become shorter and shear crack arrays become longer, ultimately resulting in similar nature of shear fracture irrespective of structural anisotropy. The differences observed in instantaneous strain of structural anisotropic classes are due to absence of fracture formation, while deformation is restricted to elastic deformation thus inferring a strong effect of structural anisotropy on formation of instantaneous strain in SPR, SPL and SPO. A similar explanation has been given by Dubey and Gairola (2000) for strength reduction in the identical structural anisotropic specimens of rocksalt deformed under cyclic loading. Similarly, the gradual reduction in transient creep phase in specimens of rocksalt can be also explained by the concept of en-echelon crack array theory (Lajtai et al., 1994; Dubey and Gairola, 2000). At lower stress levels the opening stage of inherent cracks and pore spaces will follow the structural anisotropy (orientation of bedding planes). However, at higher stresses the opening phase of inherent cracks and voids does not strictly follow the structural anisotropy, and mechanical anisotropy (cracks) evolves violently under control of stress (negligible effect and control of structural anisotropy on formation and propagation of cracks). Therefore at higher stress creep the structural anisotropy loses its control on deformation and specimens behave as mechanically isotropic rocks. The behavior of anisotropic material changes is isotropic in character when deformed at higher strain rates (see in Koyi, 1996). The textures and microstructures assisted three creep stages of rocks activated to reach the steady-state creep and accelerated creep just after crossing the elastic limit of rocksalt through changes in stress levels from low to high, without conducting the transient creep stage (like Bingham material). As a result of the process discussed above, finally the creep behavior of rocks changes as a short-term monotonic deformation (stress–strain behaviour, excluding time effect) in which rock becomes more brittle in nature and is only controlled by stress and stress-induced anisotropy. Hence the specimens exhibit steady-state creep strain just after elastic deformation of rocks (instantaneous strain) due to direct formation of shear crack arrays in all three structural anisotropic classes of rocksalt, due to weak or negligible control of structural anisotropy on deformation and assisted by development and modification of new induced anisotropy (cracks and fractures). In view of the en-echelon crack array concept (Lajtai et al., 1994; Dubey and Gairola, 2000) the lower stress creep deformation of rocks is a result of nucleation and propagation of en-echelon crack arrays (tensile crack arrays) and propagation following structural anisotropy (Fig. 10a). However, at higher stresses shear crack arrays dominate independent of the control of structural anisotropy and are under strong control of stress (Fig. 10c). Finally, all three anisotropic classes of rocksalt exhibit shear failure independent of anisotropies present in them.

5. Conclusion

The results reveal that the uniaxial compressive strength, yield strength and modulus of elasticity are higher in the case of SPR and SPL while being lower in the case of SPO. Such differences in uniaxial compressive strength are due to development of the highest induced tensile stress perpendicular to the bedding plane in SPL and maximum shear stress along the oblique bedding plane in SPO. The creep curves of SPR, SPL and SPO are non-linear with respect to time. The instantaneous strains are lower than the creep strains due to the viscoelastic nature of rocksalt. The instantaneous strain is higher in the case of SPO, intermediate in SPL and least in SPR, resulting in the time-dependent elastic constant being maximum for SPR, intermediate for SPL and minimum for SPO. Such time-dependent elastic constants are slightly lower than the modulus of elasticity determined from monotonic testing. The instantaneous strain increases with respect to increase in stress levels but the time-dependent modulus of elasticity is constant and independent of stress levels. The creep strains are pronounced in SPL and SPO in comparison to SPR, but SPO has greater fluctuation in creep strain, indicating a strong influence of structural anisotropy on creep behavior of rocksalt at lower stresses. The time limit of transient creep stage or initiation time limit of steady-state creep gradually reduces as stress level increase, and the specimens reach steady-state creep earlier than previous creeps at low stresses. The complete transient creep is lost at 70% stress level in the case of SPO, 78% stress level in the case of SPL and 80% stress level in the case of SPR. At stress level of 80% all three structural anisotropic classes of rocksalt show complete absence of transient creep stage and the steady-state creep rates are equal, irrespective of structural anisotropy. The creep of rocks is a result of evolution of tensile crack arrays and shear crack arrays in proportion. At lower stress creep the development of crack arrays is controlled by structural anisotropy, while at higher stress the shearing of rock specimens is independent of the influence of structural anisotropy.

Acknowledgments

The authors are grateful to Professor H. Koyi, Director, Hans Ramberg Tectonic Laboratory, Institute of Earth Sciences, Uppsala University, Uppsala, Sweden for his critical

comments, valuable suggestions and help for improving the scientific contents and status of research manuscript. A special thanks is also extended by the first author to Professor J.A. Hudson, Professor Imperial College, London for suggesting a variety of basic experimental approaches during the experimental stage of the investigation. The authors are thankful for the petrological microscope donated by the Alexander von Humboldt Foundation, Germany.

References

Attewel, P.B., Sandford, M.R., 1974. Intrinsic shear strength of a brittle anisotropic rock. International Journal of Rock Mechanics and Mining Sciences & Geomechanics Abstracts 11, 423–430.

Aubertin, M., Gill, D.E., Ladnyi, B., 1991. An internal variable model for the creep of rocksalt. Journal of Rock Mechanics and Rock Engineering 24, 81–97.

Aubertin, M., Sgaoula, J., Gill, D.E., 1993. A damage model for rocksalt: application of tertiary creep. In: Proceedings 7th Symposium on Salt. Elsevier, pp. 117–125.

Aubertin, M., Gill, D.E., Servant, S., 1996. Preliminary determination of constants of an updated version of SUVUC model. In: Ghoreychi, M., Berest, P., Hardy Jr., H.R., Langer, M. (Eds.), Proceedings 3rd Conference on the Mechanical Behaviour of Salt. Trans. Tech. Publications, pp. 19–30.

Badgley, P.C., 1964. Structural and Tectonics Principles. A Harper International Student Reprint. Harper & Row and John Weather Hill Inc., 1–510.

Bonini, M., 2007. Deformation patterns and structural vergence in brittle-ductile thrust wedges: An additional analogue modeling perspective. Journal of Structural Geology 29, 141–158.

Carter, N.L., Horseman, S.T., Russel, J.E., Handin, J., 1993. Rheology of rocksalt. Journal of Structural Geology 15 (9/10), 1257–1271.

Cristescu, N.D., Hunsche, U., 1998. Rock Anisotropy, Time Effects in Rock Mechanics, Wiley Series in Materials, Modeling and Computation. John Wiley and Sons, New York, pp. 65–183.

Donath, F.A,, 1964. Strength variations and deformational behaviour in anisotropic rock. In: Judd, W.R. (Ed.), State of Stress in the Earth's Crust. Elsevier, New York, pp. 281–297.

Dubey, R.K., 1996. Rheological Behaviour of Rocks of Lesser Himalaya around Mandi and Mussoorie Areas. Ph.D. Thesis. Department of Mining Engineering, B.H.U., 100 pp.

Dubey, R.K., Gairola, V.K., 2000. Influence of structural anisotropy on uniaxial compressive strength of pre-fatigued rocksalt from Himachal Pradesh, India. International Journal of Rock Mechanics and Mining Sciences & Geomechanics Abstracts 37 (6), 293–299.

Dubey, R.K., Gairola, V.K., 2005. Influence of stress rate on rheology—An experimental study on rocksalt of Simla Himalaya, India. International Journal of Geotechnical and Geological Engineering 23, 757–772.

Dubey, R.K., Nath, R., Gairola, V.K., 1999. Textural control on strength and deformation of rocksalt of Shali Formation, Simla Himalaya—an experimental approach. Rocksite, 571–576.

Dusseault, M.B., 1989. Saltrock behaviour as an analogue to the behaviour of rock at great depth. Rock At Great Depth, 11–17.

Griggs, D.T., 1939. Creep of rocks. Journal of Geology 47, 225–251.

Griggs, D.T., 1940. Experimental flow of rock under conditions favouring recrystallization. Geological Society of America 51, 1001–1022.

Griggs, D.T., Turner, F.J., Heard, H.C., 1960. Deformation of rocks at 500°C to 800°C. Geological Society of America Memoir 798, 39–104.

Hansen, F.D., 1988. Physical and mechanical variability of natural rocksalt, in: Proceedings 2nd Conference on Mechanical Behaviour of Salt, Hanover, F.G.R., Trans. Tech. Publications, pp. 23–29.

Hongliang, H.E., Ahrens, T.J., 1994. Mechanical properties of shock-damaged rocks. International Journal of Rock Mechanics and Mining Sciences & Geomechanics Abstracts 31 (5), 525–533.

Horino, F.G., Ellickson, M.L., 1970. A method for estimating strength of rock containing planes of weakness. USBM Rep. Inv. 7449, 26.

Jaroszewski, W., 1984. Fault and Fold Tectonics. Polish Scientific Publishers, Warsawa, Poland, pp. 5–12.

Kerr, P.E., 1977. Optical Mineralogy. McGraw Hill, USA, pp. 221–222.

Koyi, H., 1996. Salt flow by aggrading and prograding overburdens. In: Alsop, G.I., Blundell, D.J., Davison, I. (Eds.), Geological Society of London Special Publication 100. Salt Tectonics, pp. 243–258.

Koyi, H., 1998. The shaping of salt diapers. Journal of Structural Geology 20, 321–338.

Koyi, H., Sans, M., 2006. Deformation transfer in viscous detachments: comparison of sandbox models to South Pyrenean Triangle Zone. In: Buiter, S.J.H., Schreurs, G. (Eds.), Analogue and Numerical Modelling of Crustal-Scale Processes. Geological Society of London Special Publication, vol. 235, pp. 117–134.

Lajtai, E.Z., Carter, B.J., Duncan, E.J.S., 1994. En'echelon crack-arrays in potash salt rock. Rock Mechanics and Rock Engineering 27 (2), 89–111.

Lama, R.D., Vutukuri, V.S., 1978. Handbook on Mechanical Properties of Rocks, Vol. III. Trans Tech. Publ., pp 209–323, 383–388.

LeComte, P., 1965. Creep in rocksalt. Journal of Geology 73, 469–484.

Li, Y., Xia, C.T., 2000. Time-dependent tests on intact rocks in uniaxial compression. International Journal of Rock Mechanics and Mining Sciences & Geomechanics Abstracts 37, 467–473.

McLamore, R., Gray, K.E., 1967. The mechanical behaviour of anisotropic sedimentary rocks. Transactions of the American Society of Mechanical. Engineers Series B, 62–76.

Maranini, E., Brignoli, M., 1999. Creep behaviour of a weak rock: experimental characterization. International Journal of Rock Mechanics and Mining Sciences & Geomechanics Abstracts 36, 127–138.

Pouya, A., 1991. Correlation between mechanical behaviour and petrological properties of rocksalt. In: Roegiers, J.C. (Ed.), Rock Mechanics as a Multidisciplinary Science. Balkema, Rotterdam, pp. 385–392.

Pyrak-Nolte, P., 1996. The seismic response of fractures and the interrelation among fracture properties to seismic waves. International Journal of Rock Mechanics and Mining Sciences & Geomechanics Abstracts 33 (8), 787–802.

Ramamurthy, T., Rao, G.V., Singh, J., 1993. Engineering behaviour of phyllites. Engineering Geology 33, 209–225.

Ranalli, G., 1995. Rheology of the Earth, second ed.). Chapman and Hall, London. Chapters 1–3.

Sheorey, P.R., 1997. Empirical Rock Failure Criteria. A.A. Balkema, Oxford/IBH Publishing Co., New Delhi, pp. 61–86.

Skrotzki, W., Haasen, P., 1988. The influence of texture on the creep of salt. In: Proceedings of 2nd Conference on the Mechanical Behaviour of Salt, Hanover, F.R.G. Trans. Tech. Publications, pp. 83–86.

Suresh, S., 1998. Fatigue of Material, second ed.). Cambridge University Press, Cambridge.

Weijermars, R., 1992. Progressive deformation in anisotropic rocks. Journal of Structural Geology 14, 723–742.